RSC Advances

PAPER

View Article Online
View Journal | View Issue

Cite this: *RSC Adv.*, 2017, **7**, 14742

A novel and simple solvent-dependent fluorescent probe based on a click generated 8-aminoquinoline–steroid conjugate for multi-detection of Cu(II), oxalate and pyrophosphate†

Zhen Zhang,* Yuan Zou and Chengquan Deng

Received 8th February 2017
Accepted 28th February 2017

DOI: 10.1039/c7ra01620d

rsc.li/rsc-advances

In this work, a novel and simple deoxycholic acid-based fluorescent probe for solvent-dependent multi-detection of Cu^{2+}, $C_2O_4^{2-}$ and $P_2O_7^{4-}$ has been facilely constructed by click chemistry. This probe displayed sensitive recognition toward Cu^{2+} in low-water-content CH_3CN aqueous solution (CH_3CN–H_2O, 99/1, v/v) *via* strong fluorescence quenching. Whereas, in DMSO–H_2O medium (1/1, v/v), it exhibited significant fluorescent enhancement for $C_2O_4^{2-}$ and $P_2O_7^{4-}$ over a wide range of tested anions. Moreover, with low detection limits and fast response time, the developed fluorescent molecule was used successfully for analysis of the target ions on test paper strips and in water samples.

Introduction

The development of effective fluorescent probes for the detection of small cations, anions, and neutral molecules is of great interest and significance because of the vital roles of these species in biological, medical and environmental processes.[1–3] Conventionally, to obtain an excellent fluorescent probe, high selectivity for one analyte should be given priority in the traditional sensor design. However, the applications of these single-selective fluorescent molecules are frequently limited by their simple recognition properties resulting from the notable background interference in complicated real samples. Therefore, multi-analyte fluorescent probes, which can be regulated to bind more than one guest species with distinct spectral changes in different media based upon a single host, have gradually become an intriguing and promising research focus during the past few years.[4–17] Undoubtedly, this innovative transformation from specific to differential detection with a multi-functional probe by varying the compositions of solvent would simplify the analysis work and reduce the cost of synthesis. At present, finding novel and simple solvent-dependent fluorescent probes for multi-analyte detection is still one of the most challenging tasks.

Copper ion (Cu^{2+}) is an essential trace element in human body and serves as an important catalytic cofactor in a variety of fundamental physiological processes owing to its unique redox-active nature.[18] The levels of Cu^{2+} are firmly controlled in biological systems, as its disorders can interfere in cellular metabolism and cause many neurodegenerative diseases.[19–21] In addition, Cu^{2+} is also considered as a serious pollutant in the natural environment on account of its high toxicity. Oxalate ($C_2O_4^{2-}$) is abundantly present in nature as an important nutrient found in the human diet.[22] And it is also a primary chelator of calcium ions and forms insoluble chelates with dietary calcium, which inhibits calcium absorption in the body and is finally accumulates in the renal tissue, thus inducing renal injury, kidney lesions and pancreatic insufficiency.[23,24] As an essential anion for normal cellular function, pyrophosphate ($P_2O_7^{4-}$) involves in many crucial biochemical pathways, such as DNA and RNA polymerizations, cellular ATP hydrolysis and energy storage and transmission.[25] The difference in $P_2O_7^{4-}$ concentrations is also related to blood-clotting, telomerase activity and calcium pyrophosphate dihydrate crystal deposition disease, and therefore can be used as a potential indicator in clinical diagnosis.[26,27] Moreover, $P_2O_7^{4-}$ is one of the major phosphorus pollutants due to its wide application in our daily lives. Consequently, the development of fluorescent probes for the facile detection of Cu^{2+}, $C_2O_4^{2-}$ and $P_2O_7^{4-}$ is very important to control their concentration levels in the biosphere and avoid severe damage to humans.

Although a number of dual functional fluorescent probes for $Cu^{2+}/C_2O_4^{2-}$ and $Cu^{2+}/P_2O_7^{4-}$ have been developed,[28–38] these chemosensors for anions are always based upon the use of metal complex receptors, especially dinuclear Cu^{2+} complex, or the metal displacement approaches. Using these indirect sensing out-put methods, the detection of $C_2O_4^{2-}$ or $P_2O_7^{4-}$ is very much dependent on the design of an appropriate metal coordinative complex and the affinity of the metal ion for its complementary anion, which could be affected by various

Department of Applied Chemistry, School of Science, Xi'an Jiaotong University, Xi'an 710049, China. E-mail: zzlinda@mail.xjtu.edu.cn; Fax: +86 29 82668559; Tel: +86 29 82663914

† Electronic supplementary information (ESI) available: Experimental and spectroscopic data. See DOI: 10.1039/c7ra01620d

factors and is less easily realizable. Besides, compared to $P_2O_7^{4-}$, limited fluorescent probes for $C_2O_4^{2-}$ have been reported.[28–30,39–41] Overcoming these problems in the development of novel and simple solvent-dependent fluorescent probes that can exhibit differential optical responses in different solvent media for simultaneous and multiple detection of Cu^{2+}, $C_2O_4^{2-}$ and $P_2O_7^{4-}$ is highly desirable.

In this work, we demonstrated that a new and uncomplicated tweezer-type molecule **1** containing deoxycholic acid, 8-aminoquinoline and 1,2,3-triazole moieties could be employed as a multifunctional fluorescent probe for monitoring Cu^{2+}, $C_2O_4^{2-}$ and $P_2O_7^{4-}$ in two different solvents. As a natural product in the steroid family, deoxycholic acid can provide an ideal scaffold for receptors with its rigid framework and easily chemically-modified functional groups.[42] And 8-aminoquinoline and its derivatives are well-known excellent building blocks for constructing highly selective fluorescent sensors of transition metal cations.[36,43–46] Meanwhile, the bridging 1,2,3-triazole group was introduced *via* click chemistry in order to offer not only a straightforward strategy for the linkage of various functionalities, but also a potential binding site for both metal ions and anions,[47,48] which is very beneficial for multi-target analysis. Bearing these considerations in mind, fluorescent probe **1** was facilely synthesized by the Cu(I)-catalyzed 1,3-dipolar cycloaddition between steroidal diazides (**2**) and quinoline terminal alkyne (**3**) (Scheme 1). All the intermediates and probe **1** were well characterized (Fig. S1–S5†). The spectroscopic properties illustrated that this easily available fluorescent probe could propose a simple and sensitive solvent-dependent assay method with low detection limits and fast response time for multi-detection. Probe **1** displayed strong fluorescence quenching upon binding to Cu^{2+} in acetonitrile (CH_3CN) and water, and at the same time it exhibited remarkable fluorescence enhanced response toward $C_2O_4^{2-}$ and $P_2O_7^{4-}$ in the dimethyl sulfoxide (DMSO) aqueous solution. The practical analytical utility of the probe was also validated to determine Cu^{2+}, $C_2O_4^{2-}$ and $P_2O_7^{4-}$ on test paper strips and in water samples.

Experimental

Materials and apparatus

All chemicals were of analytical grade or higher, obtained from commercial suppliers and used without further purification. Column chromatography and thin layer chromatography were performed on silica gel (200–300 mesh) and silica gel GF254 plates, respectively. Deionized water was used for all aqueous solutions. Hydroxyethyl piperazine ethanesulfonic acid (HEPES) and sodium hydroxide were used to prepare buffer solutions. The metal ion solutions were prepared from their chloride or nitrate salts. The anion solutions were prepared from their quaternary ammonium or sodium salts.

Nuclear magnetic resonance (NMR) spectra were recorded on a Bruker Advance III 400 spectrometer. High resolution electrospray ionization mass spectrometry (HR-ESI-MS) spectra were measured on a Bruker micrOTOF-Q II mass spectrometer. Fluorescence spectra were obtained on a Hitachi F-2700 fluorescence spectrophotometer under 350 nm excitation with both excitation and emission slit widths set at 5 nm. The photomultiplier voltage was 700 V. Ultraviolet-visible (UV-vis) absorption spectra were collected on a Shimadzu UV-2700 UV-vis spectrophotometer. All pH measurements were conducted with a Mettler Toledo SG2 pH meter.

Synthesis of probe 1

Compound **2** was synthesized according to the previous ref. 49. ^{1}H NMR (400 MHz, $CDCl_3$): δ (ppm) 0.74 (s, 3H, 18-CH_3), 0.81 (d, 3H, 21-CH_3), 0.92 (s, 3H, 19-CH_3), 3.65 (s, 3H, OCH_3), 3.83 (s, 2H, –$COCH_2$), 3.88 (d, 2H, –$COCH_2$), 4.81 (m, 1H, 3-CH), 5.25 (br, 1H, 12-CH).

Compound **3** was synthesized according to the previous ref 50. ^{1}H NMR (400 MHz, $CDCl_3$): δ (ppm) 2.26 (s, 1H, ≡CH), 4.17 (s, 2H, –CH_2–), 6.43 (br, 1H, –NH–), 6.82 (d, 1H), 7.15 (d, 1H), 7.37 (m, 1H), 7.44 (m, 1H), 8.06 (d, 1H), 8.75 (d, 1H).

Synthesis of 1. To a solution of compound **2** (372 mg, 0.65 mmol) and compound **3** (260 mg, 1.43 mmol) in *tert*-butanol (30 mL) and water (2 mL), $CuCl_2 \cdot 2H_2O$ (16.6 mg, 0.098 mmol) and sodium ascorbate (77.3 mg, 0.39 mmol) were added. The resulting mixture was stirred at 65 °C for 7 h. Then the solvent was evaporated under vacuum. The residue was dissolved in dichloromethane (50 mL) and washed with saturated brine (3 × 50 mL). After being dried over anhydrous magnesium sulphate and filtered, the organic layer was condensed to dryness. The crude product was purified by column chromatography (dichloromethane–ethanol, 15/1, v/v) to afford **1** as a light yellow solid (316 mg, yield 52%). ^{1}H NMR (400 MHz, $CDCl_3$): δ (ppm) 0.66, 0.83 (2 × s, 2 × 3H, 18, 19-CH_3), 0.74 (d, 3H, 21-CH_3), 3.63

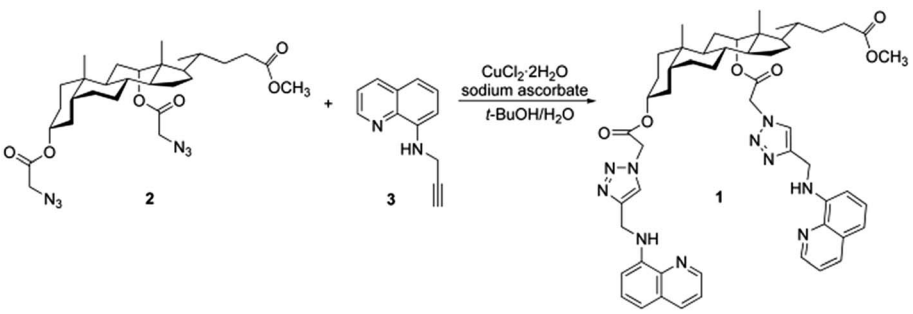

Scheme 1 The synthetic route of probe **1**.

(s, 3H, –$COOCH_3$), 4.60 (s, 2H, –$COCH_2$–), 4.70 (m, 3H, 3-H, –$COCH_2$–), 5.09 (m, 5H, –$NHCH_2$–, 12-H), 6.67 (d, 1H), 6.75 (d, 1H), 7.04 (m, 2H), 7.33 (m, 4H), 7.61, 7.65 (2 × s, 2 × 1H, triazole-H), 8.01 (m, 2H), 8.64, 8.68 (2 × dd, 2 × 1H). ^{13}C NMR (100 MHz, $CDCl_3$): δ (ppm) 12.1, 17.6, 22.6, 23.1, 25.2, 25.7, 26.0, 26.5, 27.1, 30.6, 30.8, 31.5, 33.7, 33.9, 34.4, 34.5, 35.2, 39.39, 39.43, 41.4, 44.9, 47.3, 49.2, 51.1, 51.4, 76.5, 78.3, 105.15, 105.24, 114.5, 114.6, 121.37, 121.42, 123.0, 123.3, 127.6, 127.7, 128.50, 128.51, 136.0, 137.98, 138.04, 143.97, 143.99, 146.6, 146.86, 146.89, 165.3, 165.9, 174.5. HR-ESI-MS m/z $[M + H]^+$ calcd for $C_{53}H_{65}N_{10}O_6^+$ 937.5089, found 937.5073; $[M + Na]^+$ calcd for $C_{53}H_{64}N_{10}NaO_6^+$ 959.4908, found 959.4882.

General methods for spectroscopic analysis

A stock solution of probe **1** (1 mM) was prepared in CH_3CN or DMSO, respectively. Metal ion solutions (50 mM) and anion solutions (20 mM) were prepared in deionized water. Buffer solution for tests was HEPES (10 mM). For determination of spectroscopic properties, probe **1** stock solution (1.0 mM), appropriate aliquots of organic solvent and each analyte standard solution were transferred into a microtube by a pipette and then diluted with HEPES (10 mM). All spectroscopic measurements were carried out at 25 °C with samples placed in a 1 cm path-length quartz cuvette. The relative fluorescence quantum yields for probe **1** and complexes emission in different solvents were measured using anthracene ($\Phi = 0.36$, in cyclohexane) as the quantum yield standard.[51]

Determination of the detection limit and the association constant

The detection limit was calculated from the following equation based on fluorescence titration[52]:

$$\text{Detection limit} = 3S_d/k$$

S_d is the standard deviation of blank measurements without ion tested and k is the slope between the fluorescence intensity at the maximum emission wavelength *versus* ion concentration. The fluorescence intensity of the blank probe **1** (20 μM) was measured 6 times.

The association constant (K_a) of probe **1** with ion tested was calculated from the Benesi–Hildebrand equation[53]:

$$\frac{1}{F - F_0} = \frac{1}{K_a \times (F_{eq} - F_0) \times C} + \frac{1}{F_{eq} - F_0}$$

F is the fluorescence intensity at a given ion concentration, F_0 is the fluorescence intensity in the absence of ion, and F_{eq} is the equilibrium fluorescence intensity. C is the concentration of ion added. The association constant value was determined graphically by plotting $1/(F - F_0)$ against $1/C$.

Practical application experiments

Test paper strips were prepared by immersing normal filter papers into a solution of probe **1** (1 mM) in CH_3CN or DMSO and dried in air. Then the test strips were immersed into the solutions containing different concentrations of ion tested and dried in air.

Tap water samples from different sources were freshly collected and passed through a microfiltration membrane before use. Prior to detection, the fluorescence intensity of the probe system at the maximum emission wavelength in the presence of various concentrations of ion tested was quantified under the optimized fluorescence titration conditions, and the corresponding plots were prepared as the standard curves. Then samples spiked with different concentrations of ion were quantified under the same detection conditions by fitting to the standard curves.

Results and discussion

Spectral studies of probe 1 with metal ions

First, probe **1** having nitrogen atoms of triazoles and aminoquinolines with several lone pair electrons could coordinate with metal ions, so the binding properties of probe **1** toward various metal ions, including Cu^{2+}, Fe^{2+}, Zn^{2+}, Ag^+, Hg^{2+}, K^+, Mg^{2+}, Al^{3+}, Na^+, Cr^{3+}, Ca^{2+}, Cd^{2+} and Pb^{2+}, were studied by fluorescence measurement. As shown in Fig. 1a, the free probe displayed an evident emission peak with the maximum intensity at around 470 nm ($\Phi = 0.036$) in CH_3CN–H_2O (99/1, v/v,

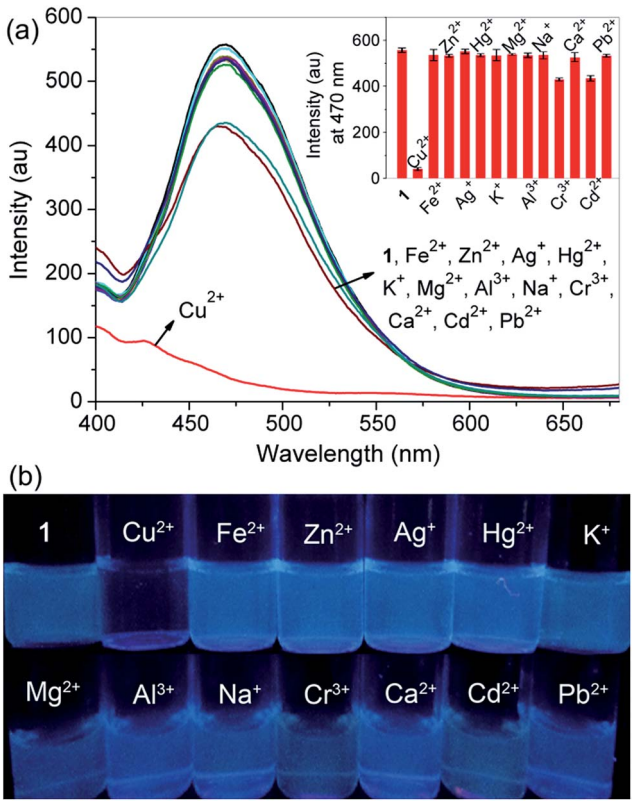

Fig. 1 (a) Fluorescence spectra of probe **1** (20 μM) with different metal ions (100 μM) in CH_3CN–H_2O (99/1, v/v, 10 mM HEPES, pH 7.2). λ_{ex} = 350 nm. Inset: fluorescence intensity of probe **1** at 470 nm with different metal ions. (b) Photographs of probe **1** (100 μM) with different metal ions (200 μM) in CH_3CN–H_2O (99/1, v/v, 10 mM HEPES, pH 7.2) taken under 365 nm illumination.

10 mM HEPES, pH 7.2), which are characteristics of the 8-aminoquinoline moiety. Upon the addition of 5.0 equivalent of Cu^{2+} into the solution of probe **1**, remarkable emission quenching was observed, while only slight decrease or a minimal change was detected for other tested metal ions under the identical conditions. The selective binding behavior of probe **1** for Cu^{2+} was also confirmed by the visual emission picture taken under 365 nm light, in which the solution color of the probe was quenched evidently from bright blue to dark black only in the presence of Cu^{2+} (Fig. 1b). The high selectivity might be attributed to the nice binding pocket for Cu^{2+} provided by triazole and aminoquinoline moieties.

During Cu^{2+} titration, a gradual decrease in the emission intensity of probe **1** solution could be visible and reached a minimum after adding 5.0 equivalent of Cu^{2+}. The observed emission maximum at 470 nm was nearly proportional to the Cu^{2+} concentration (0–5.0 equivalent), and the equilibrium fluorescence intensity was quenched about 93% of the original data (Fig. 2). The fluorescence quenching was attributed to the formation of the probe **1**–Cu^{2+} complex, resulting in the metal-to-ligand charge transfer upon excitation.[54] In this case the results are as expected because the d^9 electron configuration of Cu^{2+} usually produces a chelation enhancement of quenching (CHEQ) effect during its metal complex formation.[55] The UV-vis absorption spectrum of probe **1** was characterized by two typical absorbance bands of aminoquinoline centered at 255 (ε = 54150 M^{-1} cm^{-1}) and 355 nm (ε = 12950 M^{-1} cm^{-1}) before titration in CH_3CN–H_2O (99/1, v/v, 10 mM HEPES, pH 7.2). When Cu^{2+} was successively introduced, there was a blueshift from 255 to 230 nm, while the absorption at 355 nm gradually increased and remained constant up to the addition of 5.0 equivalent of Cu^{2+} (ε = 25500 M^{-1} cm^{-1}), and a clear isosbestic point was observed at 266 nm. These results suggested that a metal complex was generated from the binding of probe **1** with Cu^{2+} (Fig. S6†). The absorption spectra of the probe were also investigated with the aforementioned competing metal ions under the same conditions, but only slight changes were noticed, which manifested again the selectivity of probe **1** toward Cu^{2+} (Fig. S7†).

Job's plot experiments were carried out to determine the binding stoichiometry of probe **1** and Cu^{2+} under a fixed total concentration. Represented in Fig. 3a, a maximum value was

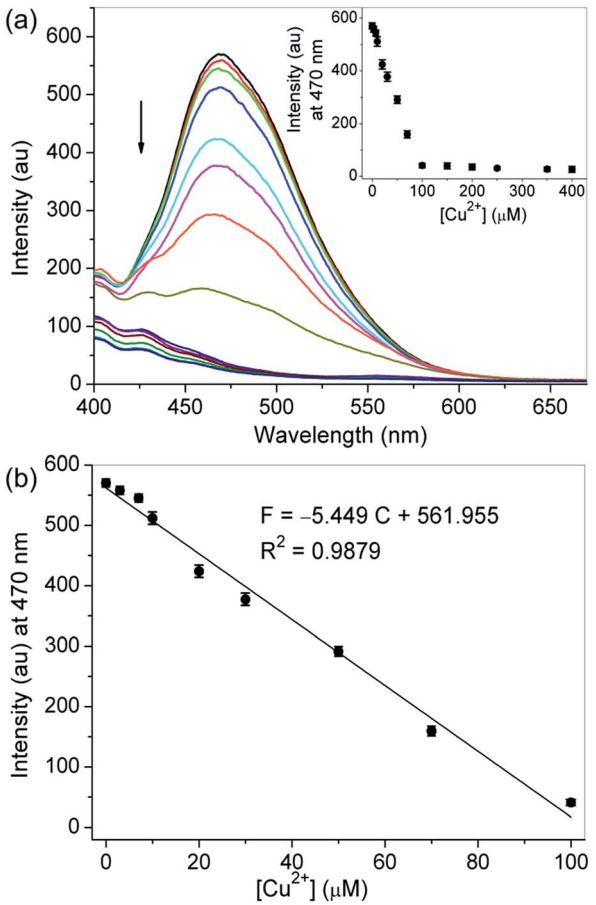

Fig. 2 (a) Fluorescence spectra of probe **1** (20 μM) with different levels of Cu^{2+} (from top to bottom: 0, 3, 7, 10, 20, 30, 50, 70, 100, 150, 200, 250, 350 and 400 μM) in CH_3CN–H_2O (99/1, v/v, 10 mM HEPES, pH 7.2). λ_{ex} = 350 nm. Inset: fluorescence intensity changes of probe **1** at 470 nm as a function of the whole range of Cu^{2+} concentration tested. (b) Fluorescence intensity changes of probe **1** at 470 nm as a function of the Cu^{2+} concentration from 0 to 100 μM.

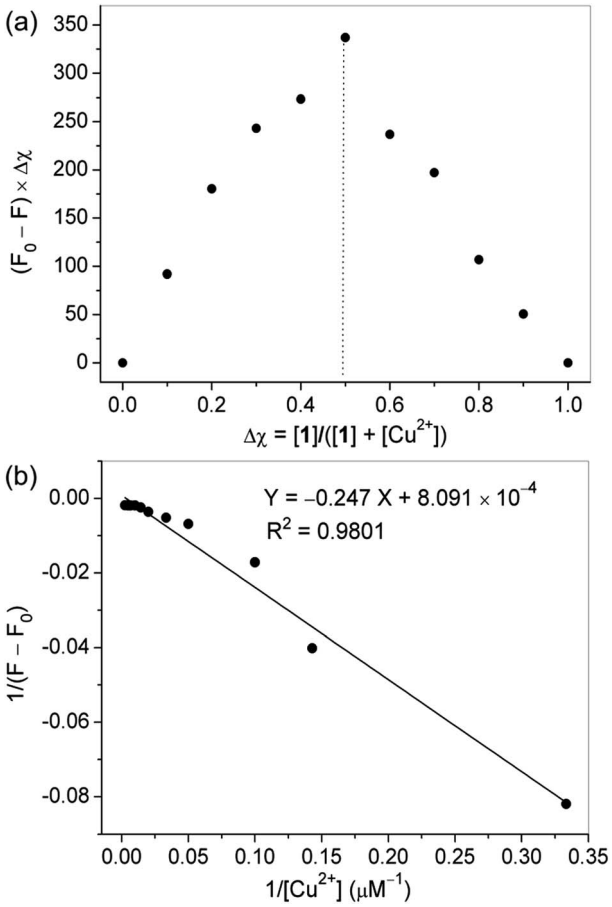

Fig. 3 (a) Job's plot from the fluorescence spectra of probe **1** and Cu^{2+} with a total concentration of 100 μM. λ_{ex} = 350 nm. (b) Benesi–Hildebrand plot from the fluorescence titration data of probe **1** (20 μM) with Cu^{2+}. The fluorescence intensity was monitored at 470 nm.

obtained when the molar fraction of probe **1** was 0.5, revealing a 1 : 1 ratio for the **1**–Cu^{2+} complex. Based on the Benesi–Hildebrand method, the association constant (K_a) of probe **1** with Cu^{2+} was calculated to be 3.28×10^3 M^{-1} (Fig. 3b). The detection limit of molecule **1** as a fluorescent probe for testing Cu^{2+} was determined to be 0.12 μM by using 20 μM probe **1** in fluorescence titration, which is reasonable for the analysis of micromolar concentrations of Cu^{2+}.

Solvent greatly affected the fluorescence emission properties of the probe and its response to Cu^{2+}. To obtain a suitable testing medium, the fluorescence emission spectra of probe **1** with Cu^{2+} were investigated in different solvents, including methanol, ethanol, *N*,*N*-dimethylformamide (DMF), DMSO and CH_3CN. Interestingly, when CH_3CN was used as the solvent, obvious and steady fluorescence quenching signals could be detected. In addition, the fluorescence response of probe **1** in the absence and presence of Cu^{2+} was found to be dependent on the ratio of CH_3CN to water (Fig. S8†). In low-water-content CH_3CN-buffer media, the probe itself gave strong fluorescent signals and efficient fluorescence quenching could be observed with the presence of Cu^{2+}. To get a better detection sensitivity and solubility of metal ion, here a CH_3CN–H_2O solution (99/1, v/v, 10 mM HEPES, pH 7.2) was chosen as the testing system to investigate the spectral characteristics of probe **1** with Cu^{2+}. The pH titration of probe **1** was performed to determine a suitable pH range for Cu^{2+} sensing (Fig. S9†). The results indicated that high-efficiency fluorescence quenching of probe **1** by Cu^{2+} was obtained in the tested pH range of 4.0–7.2, but the spectral response toward Cu^{2+} declined with the increasing pH values as a result of the hydrolysis of metal ion in basic solution. A time course study revealed that the recognizing process could complete immediately after the addition of Cu^{2+} (Fig. S10†). This feature of fast detection of Cu^{2+} is particularly favorable in practical application.

Spectral studies of probe 1 with anions

On the other hand, probe **1** having protons of acetyl methylenes, triazole rings and –NH in aminoquinolines made a very favorable platform for hydrogen bonding interactions with anions, which might change its electronic properties giving rise to an alteration of the emission properties. Hence, the recognition abilities of probe **1** toward different anions, containing $C_2O_4^{2-}$, $P_2O_7^{4-}$, F^-, Cl^-, Br^-, I^-, AcO^-, $H_2PO_4^-$, HSO_4^-, NO_3^-, CO_3^{2-}, N_3^-, S^{2-}, SCN^- and ClO_4^-, were examined by fluorescence spectroscopy. As depicted in Fig. 4a, in DMSO–H_2O (1/1, v/v, 10 mM HEPES, pH 7.2), the probe itself exhibited a characteristic emission band of 8-aminoquinoline centered at 464 nm with weaker fluorescence intensity ($\Phi = 0.024$) than in CH_3CN–H_2O (99/1, v/v, 10 mM HEPES, pH 7.2). While upon the addition of 1.5 equivalent of $C_2O_4^{2-}$ or $P_2O_7^{4-}$ into the solution of probe **1**, great fluorescence enhancement could be detectable. For other tested anions, no obvious fluorescence changes were observed under the identical conditions. The selectivity of probe **1** for $C_2O_4^{2-}$ and $P_2O_7^{4-}$ was further identified by the visual emission picture taken under 365 nm light, in which the probe showed notable turn-on responses only in the presence of

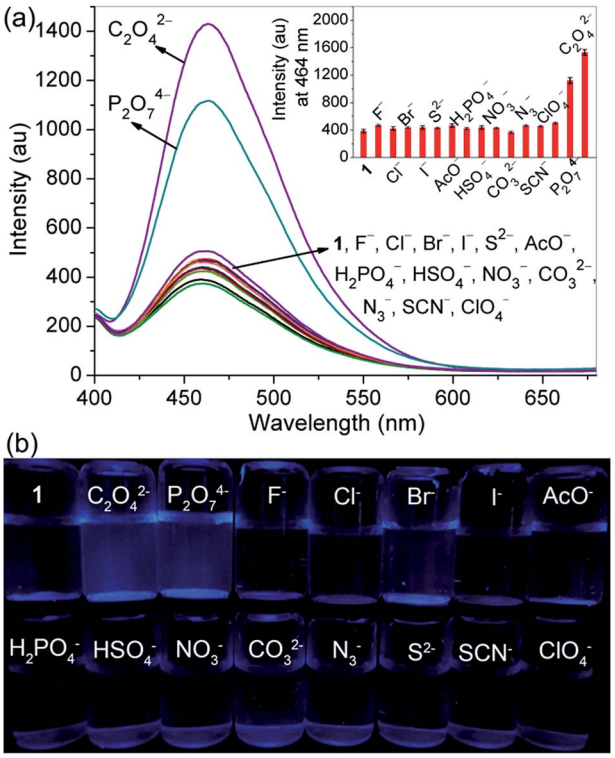

Fig. 4 (a) Fluorescence spectra of probe **1** (20 μM) with different anions (30 μM) in DMSO–H_2O (1/1, v/v, 10 mM HEPES, pH 7.2). λ_{ex} = 350 nm. Inset: fluorescence intensity of probe **1** at 464 nm with different anions. (b) Photographs of probe **1** (10 μM) with different anions (30 μM) in DMSO–H_2O (1/1, v/v, 10 mM HEPES, pH 7.2) taken under 365 nm illumination.

$C_2O_4^{2-}$ and $P_2O_7^{4-}$ (Fig. 4b). We believe that these results are related to the combined effects of both basicity and size or shape of the anions. For probe **1**, the selectivity might be due to its relatively flexible and well matched binding pocket, in which acetyl methylene protons, triazole ring protons and –NH protons of aminoquinoline could make favorable hydrogen bonding interactions with $C_2O_4^{2-}$ and $P_2O_7^{4-}$.

In the fluorescence titration profiles (Fig. 5), a gradual increase in the emission intensity of probe **1** solution could be observed with increasing $C_2O_4^{2-}$ or $P_2O_7^{4-}$ concentration until 3.5 equivalent of anion added. The emission maximum at 464 nm increased linearly with the addition of $C_2O_4^{2-}$ (0–1.5 equivalent) or $P_2O_7^{4-}$ (0–2.5 equivalent), and the equilibrium fluorescence intensity was increased 4.5 and 3.8 fold respectively. For probe **1**, the pre-organized tweezer-type scaffold with triazole rings and 8-aminoquinoline moieties might lead to the formation of a perfect hydrogen bonding cavity for accommodating $C_2O_4^{2-}$ or $P_2O_7^{4-}$. The strong complexation between the oxygen atoms of the tested two anions and the –NH groups of quinoline parts could enhance the N–H…O hydrogen bonding interaction, which resulted in the inhibition for the photo induced electron transfer (PET) process from the attached amino group to the excited singlet state of quinoline. Consequently, the fluorescence of the probe increased as the concentration of the tested anions was increased. With regard

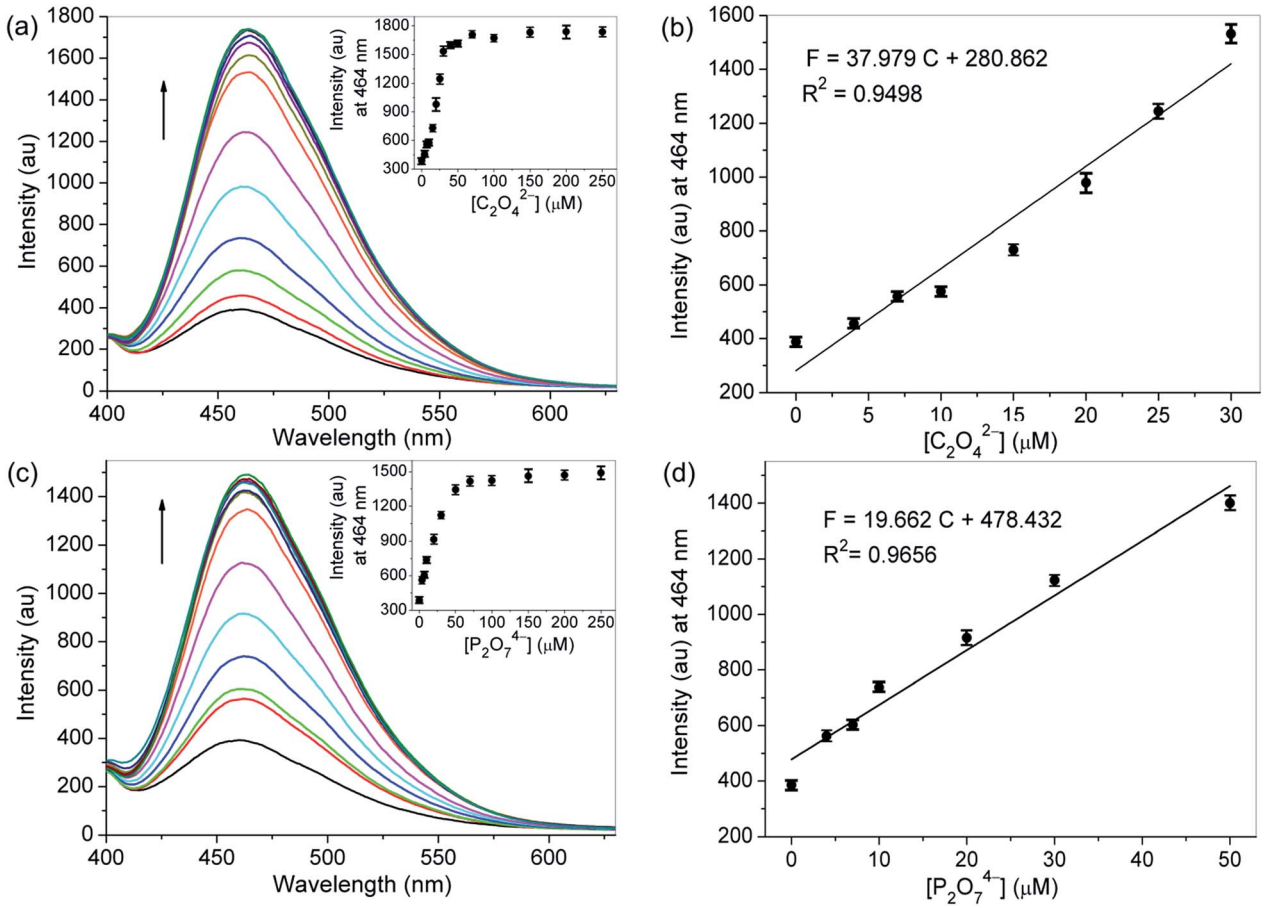

Fig. 5 Fluorescence spectra of probe **1** (20 μM) with different levels of (a) $C_2O_4^{2-}$ (from bottom to top: 0, 4, 7, 10, 15, 20, 25, 30, 40, 50, 70, 100, 150, 200 and 250 μM) and (c) $P_2O_7^{4-}$ (from bottom to top: 0, 4, 7, 10, 20, 30, 50, 70, 100, 150, 200 and 250 μM) in DMSO–H_2O (1/1, v/v, 10 mM HEPES, pH 7.2). λ_{ex} = 350 nm. Inset: fluorescence intensity changes of probe **1** at 464 nm as a function of the whole range of $C_2O_4^{2-}$/$P_2O_7^{4-}$ concentration tested. Fluorescence intensity changes of probe **1** at 464 nm as a function of (b) the $C_2O_4^{2-}$ concentration from 0 to 30 μM and (d) the $P_2O_7^{4-}$ concentration from 0 to 50 μM.

to the free probe, 11-fold and 4.2-fold quantum yields were found for the detection of $C_2O_4^{2-}$ (Φ = 0.26) and $P_2O_7^{4-}$ (Φ = 0.10) respectively. The big difference in quantum yield can be used to discriminate these two tested anions from each other. But, unlike the interaction between probe **1** and metal ions, no significant changes were observed in the bands of the absorption spectra of the probe after adding all the above-mentioned tested anions (Fig. S11 and S12†).

Job's plot experiments were carried out to determine the binding stoichiometry of probe **1** with $C_2O_4^{2-}$ or $P_2O_7^{4-}$ under a constant total concentration. As shown in Fig. 6a and c, a maximum value was obtained when the molar fraction of probe **1** was 0.5, indicating that 1 : 1 stoichiometric complexation of the probe with $C_2O_4^{2-}$ or $P_2O_7^{4-}$ was formed, respectively. Based on the fluorescence titration data, the association constant (K_a) of probe **1** for $C_2O_4^{2-}$ or $P_2O_7^{4-}$ was calculated by the Benesi–Hildebrand expression, and determined to be 2.23 × 10^4, and 4.96 × 10^4 M^{-1}, respectively (Fig. 6b and d), indicating that the probe had high binding affinities for these two anions. The detection limits of molecule **1** as a fluorescent probe for the analysis of $C_2O_4^{2-}$ and $P_2O_7^{4-}$ were calculated and found to be 0.28 and 0.55 μM, respectively, by using 20 μM probe **1** in fluorescence titration, which are appropriate for the detection of micromolar concentrations of these two ions.

To obtain suitable testing media, the fluorescence emission spectra of probe **1** with $C_2O_4^{2-}$ or $P_2O_7^{4-}$ were investigated in different solvents, including methanol, ethanol, DMF, DMSO, CH_3CN and aqueous solutions of these organic solvents. Although most of the anion recognition process was observed in non-aqueous and aprotic solvents, the results indicated that high signal turn-on ratios and better sensitivity could be obtained when the spectral properties of probe **1** with the tested two anions were investigated in an optimized mixture of DMSO–H_2O (1/1, v/v, 10 mM HEPES, pH 7.2) (Fig. S13†). The appropriate-water-content system might be able to improve the sodium salts solubility of the tested anions. The pH titration of probe **1** was performed to determine suitable pH ranges for $C_2O_4^{2-}$ and $P_2O_7^{4-}$ sensing. As depicted in Fig. S14,† high-efficiency fluorescence enhancement of probe **1** by $C_2O_4^{2-}$ or $P_2O_7^{4-}$ was observed in the tested pH range of 7.0–8.0. Time course studies revealed that the recognizing processes

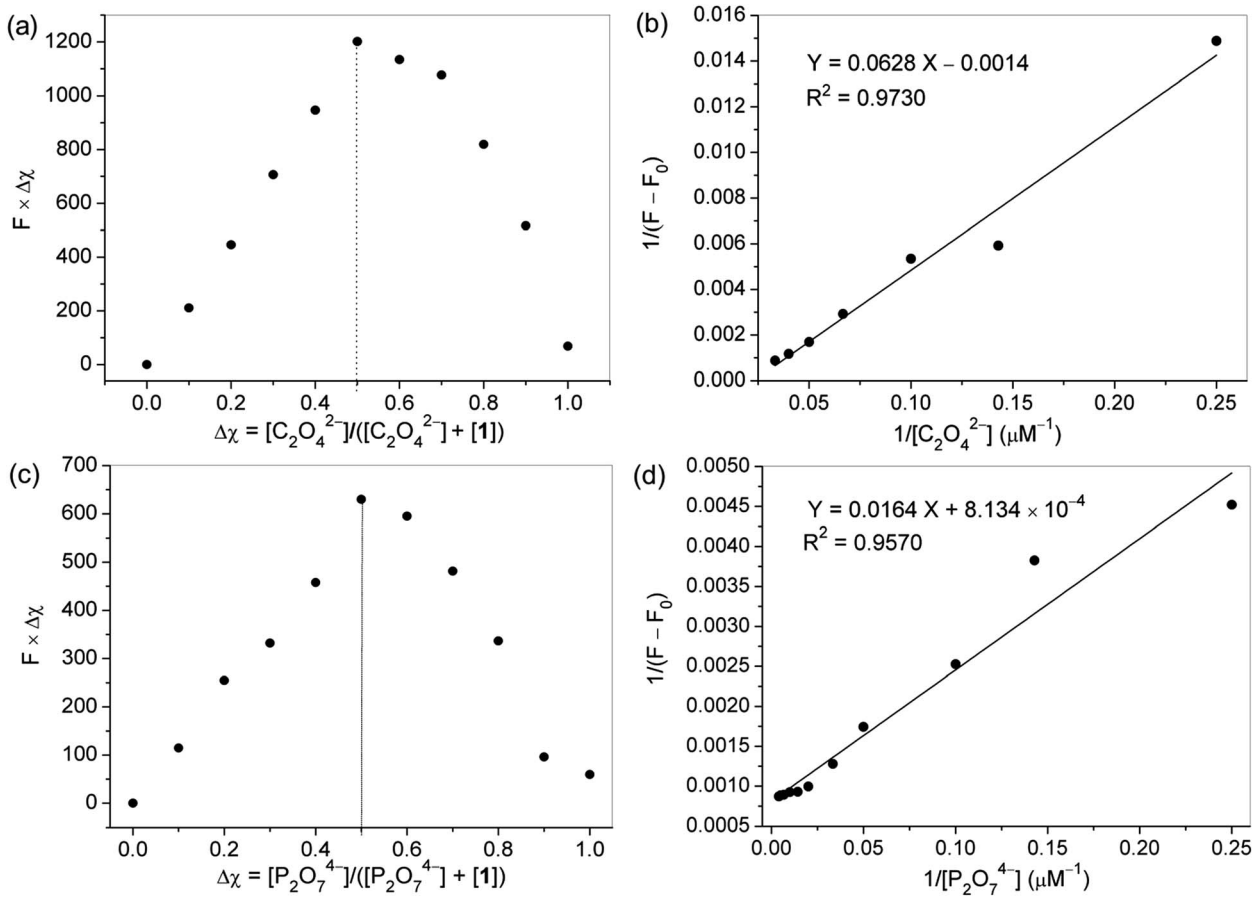

Fig. 6 Job's plot from the fluorescence spectra of (a) probe **1** and $C_2O_4^{2-}$ with a total concentration of 100 μM, and (c) probe **1** and $P_2O_7^{4-}$ with a total concentration of 50 μM. $\lambda_{ex} = 350$ nm. Benesi–Hildebrand plot from the fluorescence titration data of probe **1** (20 μM) with (b) $C_2O_4^{2-}$ and (d) $P_2O_7^{4-}$. The fluorescence intensity was monitored at 464 nm.

could complete immediately after the addition of $C_2O_4^{2-}$ or $P_2O_7^{4-}$ (Fig. S15†). The features of fast detection of $C_2O_4^{2-}$ and $P_2O_7^{4-}$ are particularly important and favorable in practical application.

Detection mechanism

To get a better understanding of the binding modes of probe **1** with Cu^{2+}, $C_2O_4^{2-}$ and $P_2O_7^{4-}$, ^{1}H NMR titration studies were performed as shown in Fig. 7 and 8.

The ^{1}H NMR spectra of probe **1** in the presence of increasing concentrations of Cu^{2+} resulted in broadening and deshielding of the proton signals of triazole units, aminoquinoline moieties as well as the two kinds of aliphatic methylenes in the tweezer-type side chains as compared to those of free probe (Fig. 7a). After the addition of 0.1 equivalent of Cu^{2+} to the solution of probe **1** (10 mM) in CD_3CN–D_2O (99/1, v/v), both triazole protons (H_2) showed slight downfield shifts by 0.025 and 0.055 ppm, respectively. Besides, slight downfield shifts in H_6 of aminoquinoline moieties by 0.020 and 0.030 ppm, respectively, along with deshielding of methylene protons (H_1 and H_3) by 0.015 ppm suggested the crucial roles of 1,2,3-triazole rings and aminoquinoline groups as binding sites in the recognition of Cu^{2+}. Due to the

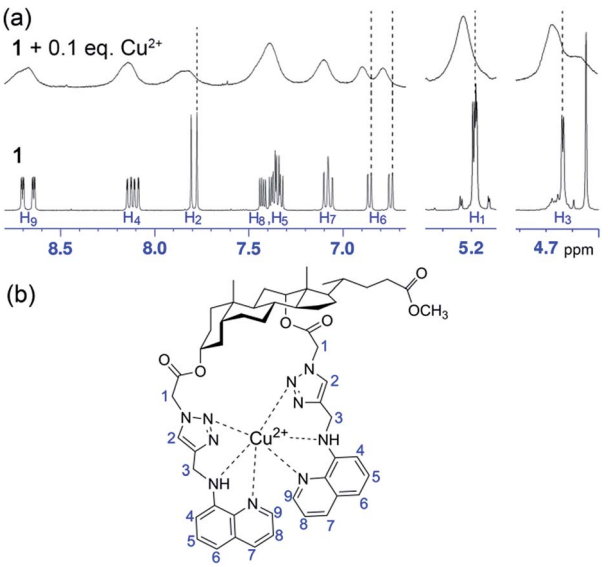

Fig. 7 (a) Partial ^{1}H NMR spectra of probe **1** (10 mM) measured before and after addition of Cu^{2+} (0.1 equivalent) in CD_3CN–D_2O (99/1, v/v). (b) The proposed binding mode between probe **1** and Cu^{2+}.

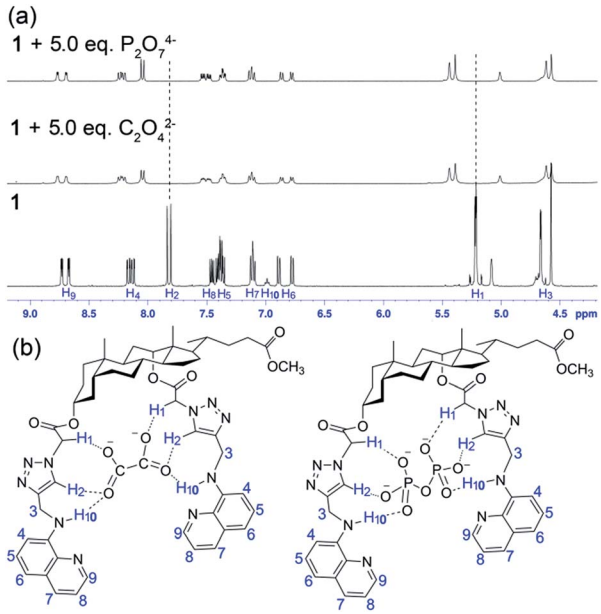

Fig. 8 (a) Partial ^{1}H NMR spectra of probe **1** (10 mM) measured before and after addition of $C_2O_4^{2-}$ or $P_2O_7^{4-}$ (5.0 equivalent) in deuterated DMSO–D_2O (19/1, v/v). (b) The proposed binding interactions between probe **1** and anions.

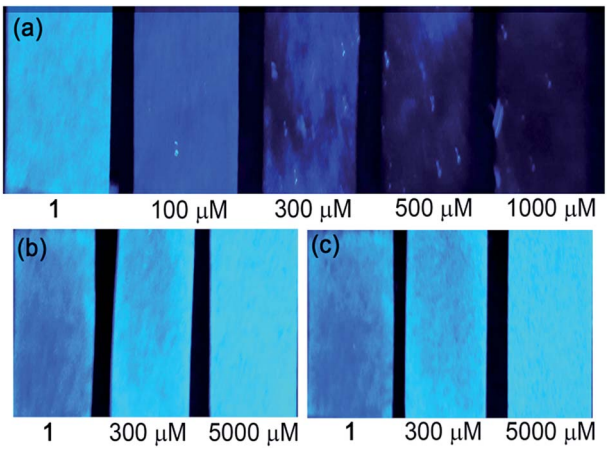

Fig. 9 Photographs of test paper strips containing probe **1** (1 mM) for detection of (a) Cu^{2+}, (b) $C_2O_4^{2-}$ and (c) $P_2O_7^{4-}$ with different concentrations under 365 nm illumination.

paramagnetic property of Cu^{2+}, the protons of steroidal skeleton moiety and methylenes in the tweezer-type side chains (H_1 and H_3) became more broadened, while the protons of triazole and aminoquinoline groups (H_2, H_4–H_9) disappeared completely even in the presence of 0.5 equivalent of Cu^{2+} (Fig. S16†). The reversible binding ability of probe **1** toward Cu^{2+} was verified by introduction of ethylenediaminetetraacetic acid disodium salt (EDTA-2Na) into the system containing probe **1** (20 μM) and Cu^{2+} (100 μM). The experiment results showed that the completed quenched fluorescence signal of probe **1** by Cu^{2+} was recovered gradually with the addition of increasing concentrations of EDTA (Fig. S17†). Based on the spectral and ^{1}H NMR data, a tentative binding mode between probe **1** and Cu^{2+} is presented in Fig. 7b.

The ^{1}H NMR titration of probe **1** with $C_2O_4^{2-}$ and $P_2O_7^{4-}$ illustrated the involvement of protons in anion binding. As shown in Fig. 8a, upon the addition of 5.0 equivalent of $C_2O_4^{2-}$ or $P_2O_7^{4-}$ to the solution of probe **1** (10 mM) in deuterated DMSO–D_2O (19/1, v/v), downfield shifts of triazole protons (H_2, 7.80–8.02 and 7.84–8.04 for $C_2O_4^{2-}$, and 7.80–8.01 and 7.84–8.03 for $P_2O_7^{4-}$) and acetyl methylene protons (H_1, 5.21–5.37 and 5.21–5.44 for both $C_2O_4^{2-}$ and $P_2O_7^{4-}$) were observed, respectively. And the proton signals of –NH at 7.0 ppm (H_{10}) in aminoquinoline moieties became invisible after addition of the tested two anions, presumably as a result of broadening by hydrogen bond interactions. The quinoline ring protons H_4 and H_9 showed slight downfield shifting on complexation. These clearly indicated the participation of triazole protons, H_1 methylene protons as well as –NH protons in the hydrogen bonding with $C_2O_4^{2-}$ and $P_2O_7^{4-}$. The reversible binding abilities of probe **1** toward $C_2O_4^{2-}$ and $P_2O_7^{4-}$ were verified by introduction of Pb^{2+} into the probe–anion complex system. The experiment results demonstrated that the enhanced fluorescence of probe **1** by $C_2O_4^{2-}$ or $P_2O_7^{4-}$ was quenched gradually with the addition of increasing concentrations of Pb^{2+}, while the addition of Pb^{2+} to the solution of probe **1** alone did not cause obvious change under the identical conditions, suggesting that the presence of Pb^{2+} quenched the fluorescence of the probe–anion complex through the formation of insoluble salts between Pb^{2+} and the tested anion, and therefore the probe–anion complexation was reversible (Fig. S18†). The proposed binding interactions between probe **1** and anions are given in Fig. 8b according to the spectral and ^{1}H NMR data.

Analytical application

To investigate the practical applications of the probe, experiments for visual detection of Cu^{2+}, $C_2O_4^{2-}$ and $P_2O_7^{4-}$ on solid paper strips with naked eyes under 365 nm light were first performed. As shown in Fig. 9, remarkable color changes of the paper strips containing probe **1** (1 mM) appeared clearly from bright blue to dark black upon interaction with different levels of Cu^{2+} (0, 100, 300, 500, 1000 μM) under UV light. Interestingly, the color of the paper strips containing probe **1** (1 mM) showed immediate and sensitive changes from dark blue to light blue after interaction with $C_2O_4^{2-}$ or $P_2O_7^{4-}$ (0, 300, 5000 μM) under UV light. The utilization of these dipsticks is particularly useful as an instant qualitative method without resorting to instrumental analysis.

The probe was also applied to the detection of our target ions in tap water samples. Before the experiments, the corresponding calibration plots were prepared as the standard curves under the optimized fluorescence titration conditions. No significant fluorescence changes were produced with both tap water samples, indicating that these samples are free from detectable amount of target ions. The recovery studies were further conducted by spiking two different concentrations of Cu^{2+}, $C_2O_4^{2-}$ or $P_2O_7^{4-}$ in triplicate to both the samples. The

Table 1 Recovery of Cu^{2+}, $C_2O_4^{2-}$ and $P_2O_7^{4-}$ in spiked water samples[a]

		Tap water 1		Tap water 2	
Ions	Spiked (μM)	Found (μM)	Recovery (%)	Found (μM)	Recovery (%)
Cu^{2+}	10	10.26 ± 0.11	102.6	11.13 ± 0.21	111.3
	30	29.44 ± 0.13	98.1	29.52 ± 0.19	98.4
$C_2O_4^{2-}$	10	10.06 ± 0.39	100.6	9.63 ± 0.10	96.3
	25	24.60 ± 0.32	98.4	24.50 ± 0.37	98.0
$P_2O_7^{4-}$	10	9.86 ± 0.25	98.6	10.20 ± 0.33	102.0
	25	24.46 ± 0.69	97.8	25.15 ± 0.14	100.6

[a] Mean ($n = 3$) ± standard deviation.

good percentage recoveries proved the fine accuracy of this fluorescent system and its potential applicability in environmental water (Table 1).

Conclusions

In summary, a novel and simple deoxycholic acid-based fluorescent probe for multi-detection of Cu^{2+}, $C_2O_4^{2-}$ and $P_2O_7^{4-}$ in different media has been facilely constructed using Cu(I)-catalyzed click reaction of steroidal azides and quinoline terminal alkyne. In this molecule, binding sites and the fluorophore subunits are covalently bonded to form a relatively flexible binding cleft, in which nitrogen atoms of triazoles and aminoquinolines provided a matched binding pocket for Cu^{2+} with strong fluorescence quenching in CH_3CN aqueous solution, while protons of acetyl methylenes, triazole rings and –NH in aminoquinolines made favorable hydrogen bonding interactions with $C_2O_4^{2-}$ and $P_2O_7^{4-}$ accompanied by obvious fluorescence enhancement in DMSO aqueous solution. With high sensitivity, low detection limits and fast response time, this fluorescent probe also showed good performance of determination on test paper strips and in water samples. Compared with the recently reported multi-detection probes for Cu^{2+}, $C_2O_4^{2-}$ and $P_2O_7^{4-}$ (Table S1†), our report is the first single fluorescent molecule to our knowledge that can separately detect them with distinct emission in different solvents. The design strategy of the molecule will be helpful in developing fluorescent probes for multi-analyte response, thus probably providing further insight into how to construct efficient sensors with special properties.

Acknowledgements

This work is supported by the National Natural Science Foundation of China (21102112), the Scientific and Technological Development Project of Shaanxi Province (2015GY148), and the Fundamental Research Funds for the Central Universities.

Notes and references

1 X. Chen, F. Wang, J. Y. Hyun, T. Wei, J. Qiang, X. Ren, I. Shin and J. Yoon, *Chem. Soc. Rev.*, 2016, **45**, 2976–3016.
2 J. Yin, Y. Hua and J. Yoon, *Chem. Soc. Rev.*, 2015, **44**, 4619–4644.
3 T. D. Ashton, K. A. Jolliffe and F. M. Pfeffer, *Chem. Soc. Rev.*, 2015, **44**, 4547–4595.
4 L. Li, Y. Shen, Y. H. Zhao, L. Mu, X. Zeng, R. Carl and G. Wei, *Sens. Actuators, B*, 2016, **226**, 279–288.
5 X. Li, Y. Yin, J. Deng, H. Zhong, J. Tang, Z. Chen, L. Yang and L. J. Ma, *Talanta*, 2016, **154**, 329–334.
6 L. He, C. Liu and J. H. Xin, *Sens. Actuators, B*, 2015, **213**, 181–187.
7 Z. Yang, M. She, B. Yin, L. Hao, M. Obst, P. Liu and J. Li, *Anal. Chim. Acta*, 2015, **868**, 53–59.
8 Y. Chen, Q. Lv, Z. Liu and Q. Fang, *Inorg. Chem. Commun.*, 2015, **52**, 38–40.
9 X. Fang, S. Zhang, G. Zhao, W. Zhang, J. Xu, A. Ren, C. Wu and W. Yang, *Dyes Pigm.*, 2014, **101**, 58–66.
10 P. S. Hariharan, N. Hari and S. P. Anthony, *Inorg. Chem. Commun.*, 2014, **48**, 1–4.
11 J. Y. Noh, S. Kim, I. H. Hwang, G. Y. Lee, J. Kang, S. H. Kim, J. Min, S. Park, C. Kim and J. Kim, *Dyes Pigm.*, 2013, **99**, 1016–1021.
12 M. Yu, R. Yuan, C. Shi, W. Zhou, L. Wei and Z. Li, *Dyes Pigm.*, 2013, **99**, 887–894.
13 S. Goswami, S. Maity, A. K. Das and A. C. Maity, *Tetrahedron Lett.*, 2013, **54**, 6631–6634.
14 Y. Chen, Y. Mi, Q. Xie, J. Xiang, H. Fan, X. Luo and S. Xia, *Anal. Methods*, 2013, **5**, 4818–4823.
15 T. Cheng, T. Wang, W. Zhu, Y. Yang, B. Zeng, Y. Xu and X. Qian, *Chem. Commun.*, 2011, **47**, 3915–3917.
16 Y. Liu, Y. Sun, J. Du, X. Lv, Y. Zhao, M. Chen, P. Wang and W. Guo, *Org. Biomol. Chem.*, 2011, **9**, 432–437.
17 L. Xu, Y. Xu, W. Zhu, B. Zeng, C. Yang, B. Wu and X. Qian, *Org. Biomol. Chem.*, 2011, **9**, 8284–8287.
18 R. Uauy, M. Olivares and M. Gonzalez, *Am. J. Clin. Nutr.*, 1998, **67**, 952S–959S.
19 L. M. Gaetke and C. K. Chow, *Toxicology*, 2003, **189**, 147–163.
20 Y. H. Hung, A. I. Bush and R. A. Cherny, *J. Biol. Inorg. Chem.*, 2010, **15**, 61–76.
21 J. C. Lee, H. B. Gray and J. R. Winkler, *J. Am. Chem. Soc.*, 2008, **130**, 6898–6899.
22 A. Jajoo, A. Sahay, P. Singh, S. Mathur, S. K. Zharmukhamedov, V. V. Klimov, S. I. Allakhverdiev and S. Bharti, *Photosynth. Res.*, 2008, **97**, 177–184.

23 E. L. Greene, G. Farell, S. H. Yu, T. Matthews, V. Kumar and J. C. Lieske, *Urol. Res.*, 2005, **33**, 340–348.
24 F. T. Borges, Y. M. Michelacci, J. A. K. Aguiar, M. A. Dalboni, A. S. Garofalo and N. Schor, *Kidney Int.*, 2005, **68**, 1630–1642.
25 M. Ronaghi, S. Karamohamed, B. Pettersson, M. Uhlen and P. Nyren, *Anal. Biochem.*, 1996, **242**, 84–89.
26 A. E. Timms, Y. Zhang, R. G. G. Russell and M. A. Brown, *Rheumatology*, 2002, **41**, 725–729.
27 M. Doherty, C. Becher, M. Regan, A. Jones and J. Ledingham, *Ann. Rheum. Dis.*, 1996, **55**, 432–436.
28 S. Zhang, Q. Wang, G. Tian and H. Ge, *Mater. Lett.*, 2014, **115**, 233–236.
29 M. Hu and G. Feng, *Chem. Commun.*, 2012, **48**, 6951–6953.
30 L. Tang, J. Park, H. J. Kim, Y. Kim, S. J. Kim, J. Chin and K. M. Kim, *J. Am. Chem. Soc.*, 2008, **130**, 12606–12607.
31 J. Qiang, C. Chang, Z. Zhu, T. Wei, W. Yu, F. Wang, J. Yin, Y. Wang, W. Zhang, J. Xie and X. Chen, *Sens. Actuators, B*, 2016, **233**, 591–598.
32 G. Wang, H. Chen, Y. Chen and N. Fu, *Sens. Actuators, B*, 2016, **233**, 550–558.
33 C. Zhao, B. Liu, X. Bi, D. Liu, C. Pan, L. Wang and Y. Pang, *Sens. Actuators, B*, 2016, **229**, 131–137.
34 Z. S. Qian, L. J. Chai, Y. Y. Huang, C. Tang, J. J. Shen, J. R. Chen and H. Feng, *Biosens. Bioelectron.*, 2015, **68**, 675–680.
35 W. Yu, J. Qiang, J. Yin, S. Kambam, F. Wang, Y. Wang and X. Chen, *Org. Lett.*, 2014, **16**, 2220–2223.
36 L. Tang, P. Zhou, Z. Huang, J. Zhao and M. Cai, *Tetrahedron Lett.*, 2013, **54**, 5948–5952.
37 X. J. Zhao and C. Z. Huang, *Biosens. Bioelectron.*, 2011, **30**, 282–286.
38 L. Tang, M. Liu, F. Li and R. Nandhakumar, *J. Fluoresc.*, 2011, **21**, 701–705.
39 G. Wang, H. Zhu, Y. Lin, Y. Chen and N. Fu, *Sens. Actuators, B*, 2015, **206**, 624–629.
40 L. Tang, D. Wu, X. Wen, X. Dai and K. Zhong, *Tetrahedron*, 2014, **70**, 9118–9124.
41 C. He, X. Qian, Y. Xu, C. Yang, L. Yin and W. Zhu, *Dalton Trans.*, 2011, **40**, 1034–1037.
42 S. Banerjee, R. K. Das and U. Maitra, *J. Mater. Chem.*, 2009, **19**, 6649–6687.
43 R. Shen, D. Liu, C. Hou, J. Cheng and D. Bai, *Anal. Methods*, 2016, **8**, 83–88.
44 J. Huang, Y. Xua and X. Qian, *Dalton Trans.*, 2014, **43**, 5983–5989.
45 R. Alam, T. Mistri, A. Katarkar, K. Chaudhuri, S. K. Mandal, A. R. K. Bukhsh, K. K. Das and M. Ali, *Analyst*, 2014, **139**, 4022–4030.
46 Z. Dong, X. Le, P. Zhou, C. Dong and J. Ma, *New J. Chem.*, 2014, **38**, 1802–1808.
47 Y. H. Lau, P. J. Rutledge, M. Watkinson and M. H. Todd, *Chem. Soc. Rev.*, 2011, **40**, 2848–2866.
48 J. Hu, J. R. Lu and Y. Ju, *Chem.–Asian J.*, 2011, **6**, 2636–2647.
49 J. Wu, Y. Gao, J. Lu, J. Hu and Y. Ju, *Sens. Actuators, B*, 2015, **206**, 516–523.
50 Y. M. Zhang, Y. Chen, Z. Q. Li, N. Li and Y. Liu, *Bioorg. Med. Chem.*, 2010, **18**, 1415–1420.
51 H. Du, R. A. Fuh, J. Li, A. Corkan and J. S. Lindsey, *Photochem. Photobiol.*, 1998, **68**, 141–142.
52 Y. Qian, L. Cao, C. Jia, P. O. Boamah, Q. Yang, C. Liu, Y. Huang and Q. Zhang, *RSC. Adv.*, 2015, **5**, 77965–77972.
53 J. R. Lin, C. J. Chu, P. Venkatesan and S. P. Wu, *Sens. Actuators, B*, 2015, **207**, 563–570.
54 E. Hao, T. Meng, M. Zhang, W. Pang, Y. Zhou and L. Jiao, *J. Phys. Chem. A*, 2011, **115**, 8234–8241.
55 B. Pedras, V. Rosa, R. Welter, C. Lodeiro and T. Avilés, *Inorg. Chim. Acta*, 2012, **381**, 143–149.